4th Conference on Production Systems and Logistics

Application-Oriented Method For Determining The Adhesion between Insulated Flat Copper Wire And Impregnation Resin

Achim Kampker[1], Heiner Hans Heimes[1], Benjamin Norbert Dorn[1], Florian Brans[1], Henrik Christoph Born[1]

[1]*Chair of Production Engineering of E-Mobility Components, RWTH Aachen University, Aachen, Germany*

Abstract

In the field of hairpin stator technology, increasing demands are currently being made on the semi-finished product of insulated flat copper wire. In particular, the focus is on the electrical requirements against the background of increasing voltage levels to 800 V and more. The test procedures described in the standards IEC 60317 & 60851 for verifying the properties of insulated flat copper wires only partially map the requirements from the point of automotive industry. An example for insufficiently considered properties lays in the correlation between wire and insulation resin. In addition to electrical and thermal benefits, impregnation helps to mechanically stabilize the winding and protect it from ambient factors. Adhesion between the winding and the impregnating resin is a key parameter here but is not considered in material pre-selection today. The adhesion of the impregnation resin to the insulated wire is essential to ensure the lifetime of electric motors. This paper describes a method for determining the adhesion of the impregnating resin to the insulation of the wire. It could be shown that there is a correlation between the material of the wire insulation and the impregnating resin in terms of adhesion. Further on the described method can be used for an application-oriented specification of insulated copper flat wires to ensure a consistent composition of the insulation material.

Keywords

Hairpin stator technology; Electric motor production; Secondary insulation; Flat copper wire; Impregnation; 800V; Test procedure; PAI; PEEK

1. Introduction

While hairpin stator technology is still in the ramp-up phase, the next wave of product-side optimization is already emerging with 800 V technology and the use of SiC-based semiconductors in power electronics. The significantly higher voltages - coupled with higher switching frequencies - are accompanied by higher requirements for insulation systems along the entire electrical drivetrain. [1,2] These also affect the insulation material on insulated copper flat wires in hairpin applications. To meet the increased requirements, the hairpin sector is working towards thicker layers, but also more and more towards alternative insulation materials. While polyamide-imide (PAI) is the most common material in automotive traction drives, other insulation materials such as polyetheretherketone (PEEK) or perfluoroalkoxy polymers (PFA) are also used.

In the context of the electric motor, wire insulation is also referred to as primary insulation. Secondary insulation involves, besides the insulation paper, impregnation of the stator winding. In one of the later process steps within the stator production process the wound stator is impregnated by a trickling or dipping

DOI: https://doi.org/10.15488/13494
ISSN: 2701-6277

process. The impregnation process contains a sub-process in which the stator winding is cast with a liquid resin, which hardens under the influence of heat in the second sub-process. [3] The impregnation serves to mechanically fix the winding and optimize the insulation and thermal conductivity properties of the insulation system by casting the wire gaps. In the process, capillary action causes the liquid resin to penetrate and fill the wire gaps in the stator slots. [4]

By optimizing the properties of the electrical insulation and the thermal conductivity of the stator insulation system, impregnation leads to an increase in the service life of the entire stator. A decisive quality feature in this context is the filling factor, especially at the bottom of the slot and between the windings. A faulty process causes cavities, which can lead to premature stator failure due to the increasing probability of partial discharges or electrical breakdowns (cf. Figure 1) [5].

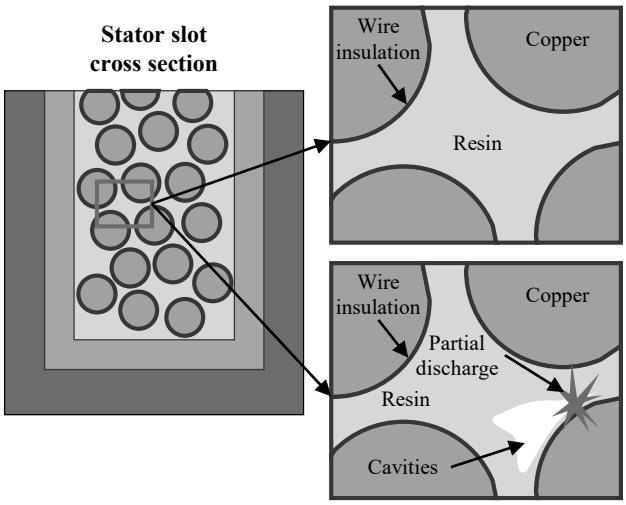

Figure 1: Quality features of impregnated stator windings

The impregnation resin as the secondary insulation interacts directly with the insulation material on the copper flat wire as the primary insulation. To ensure a sufficient fill factor in the spaces between the windings, the adhesion between the wire insulation and the resin is also decisive. For long-lasting operation of the electric motor, it is also crucial that the resin does not detach from the insulation material due to vibrations during operation, as damage in this insulation system can also lead to failure of the drive unit.

Against this background, the interaction in the form of adhesion between insulated flat copper wire and the impregnation resin must be investigated for different material combinations. Up to now, there has been no standardized test method for quantifying the adhesion in a reproducible manner. The common standards IEC 60317 and 60851 for winding wires do not consider this property [6,7]. The test procedure described below represents an approach to measuring adhesion between the two insulation materials. In this way, material combinations are to be investigated with regard to adhesion, so that the best material combination for wire insulation and impregnation resin can be selected. In perspective, the transfer of this method e.g., into a material specification as well as for quality control is suitable to ensure application-oriented properties of flat copper wires and impregnation resins.

2. Methodology

2.1 Experimental setup

The overall objective is to determine the adhesion between the impregnating resin and the insulation of the copper wire. The force with which a cylinder of resin can be pulled off a wire sample represents the central

measured variable. With this measurand, differences in the adhesion of the impregnating resin to the insulation layer are to be identified and made measurable.

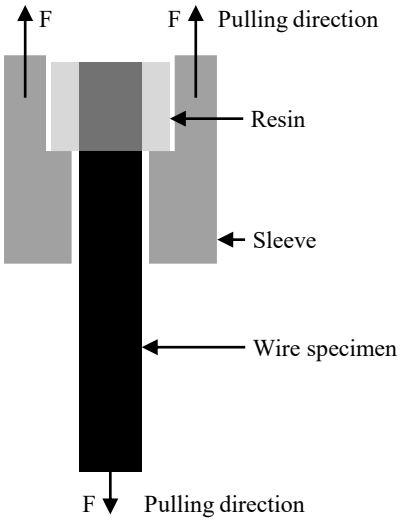

Figure 2: Schematic illustration of the test procedure

The experimental setup of the test is shown in Figure 2. The wire specimen is coated with impregnation resin at one end. In order to clamp the specimen in a tensile testing machine, a sleeve is placed directly against the hardened resin. This allows a tensile force to be applied to the resin in a subsequent tensile test. The sleeve is made of steel and is clamped in the tensile testing machine. As a result, the cured impregnation resin is not affected by shear forces. Since the cured resin is very brittle, there would otherwise be a risk that the shear forces would damage it.

2.2 Preparation of specimen

The process for producing the specimens is divided into four main steps, which are shown schematically in Figure 3. In the first step, a mold is 3D printed which contains the positive shape of the specimen to be cast later. For the later demoldability of the parts to be cast, demolding chamfers are provided on the flanks. In the second step, this mold is filled with a silicone. Curing of the silicone creates a negative mold, in which the actual specimens for the test are cast in the next step. An addition-curing silicone (Wacker Elastosil® RT 620 A/B [8]) was used to make the silicone molds. The advantage of this material is that it vulcanizes quickly and without shrinkage at room temperature. Meanwhile, vulcanization can be significantly accelerated by applying heat. In the context of the production of the silicone molds, vulcanization took place at 60 °C in the oven. In order to prevent the 3D printed molds from melting at this temperature, they were manufactured using stereolithography, since the material used loses its mechanical properties at significantly higher temperatures. It would also be conceivable to manufacture the 3D printed molds using fused filament fabrication (FFF), but the silicone can then only vulcanize at room temperature, which is time-consuming.

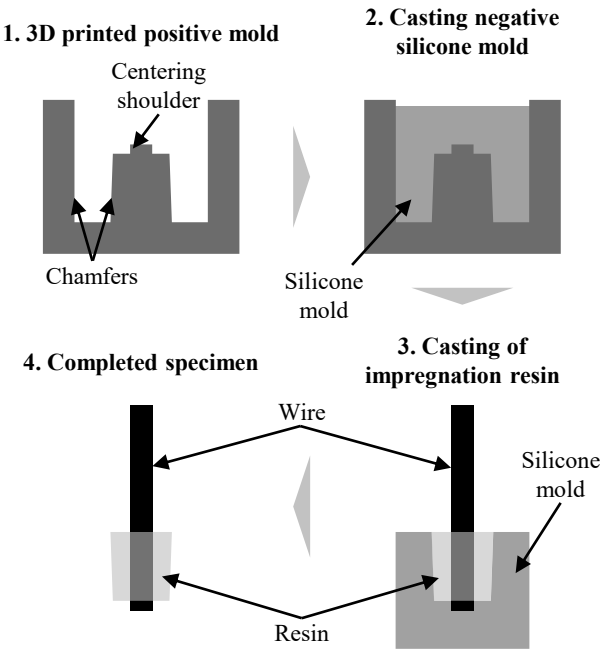

Figure 3: Schematic procedure for the preparation of the specimen

The 3D printed molds are provided with a small shoulder on the middle cylinder, which exactly corresponds to the wire cross-section. This shoulder results in a recess in the silicone mold, which serves to center the wire used exactly in the silicone mold during the production of the wire specimen. As a result, new molds must be made for each wire cross section used. However, due to the low material costs of the molds, the advantages resulting from the possibility of exact centering outweigh dis disadvantage.

In order to produce several wire specimens simultaneously, a jig was designed and manufactured, which is shown in Figure 4. The lower, laser-cut sheet contains cutouts in which the silicone molds can be placed and clearly define their position. The upper sheet also has cutouts that correspond exactly to the wire cross-section. The cutouts in the upper sheet serve both to fix the wires and to center the wire sample in the silicone mold. The cutouts in the sheet are exactly above the previously mentioned shoulder in the silicone molds, so that the wire is positioned exactly centered and straight in the silicone mold.

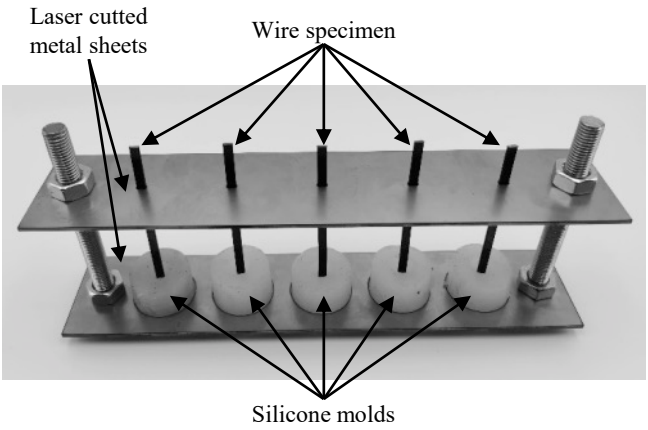

Figure 4: Setup for the production of multiple wire samples

After positioning the wires in the build-up, the silicone molds are filled with impregnation resin. The entire assembly is then placed in an oven, for curing of the impregnation resin. The temperature of the oven as well as the time for curing depends on the resin used.

After the resin has cured in the oven, the specimens are demolded. This is where the advantage of silicone becomes apparent. Due to the soft properties of the silicone, it can be separated from the resin with little force, so that neither the specimen nor the mold is damaged. The finished specimen is shown in Figure 5.

Figure 5: Finished wire sample with cured resin

2.3 Execution of tests

The specimens are clamped on a tensile testing machine as shown in Figure 6. In the starting position, the distance between the clamping jaws is 25 mm. The turned sleeve is clamped over its complete length with the clamping jaws. For a total specimen length of 90 mm, the length of the clamping of the wire is 40 mm.

The specimen is pulled at a test speed of 100 mm/min. The test ends as soon as the test force drops, as it can be assumed that the impregnating agent detaches from the wire at this point. The maximum measured force is noted as the force at which the impregnating agent detaches from the wire and is thus the relevant measurand for determining the adhesion between resin and insulated flat copper wire.

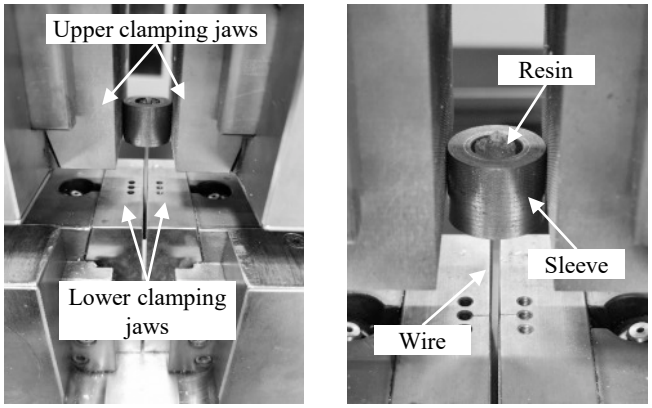

Figure 6: Test setup on tensile testing machine

3. Results and Discussion

In the following the results of the tests are presented and discussed. The tests were performed with three different flat wires. The properties of the flat wires are shown in Table 1. For the impregnation resin, a material from the company Elantas© (ELAN-protect® UP142 [9]) was used. This resin is widely used in the production of electric motors and hairpin stators.

Table 1: Characteristics of the flat wires used for the tests

Name	Dimensions [mm x mm]	Insulation thickness [µm]	Insulation material
PAI 1	4,00 x 1,50	80	PAI
PAI 2	3,64 x 2,59	100	PAI
PEEK	3,90 x 1,80	100	PEEK

First, the measurement results of the maximum force according to the wire used are shown in a box plot. Based on this, the functionality and informative value of the developed test procedure is assessed. Subsequently, three force-elongation curves per wire used are compared with each other as examples in order to analyze and interpret the measurement results for the individual wire insulation materials.

For each of the three wires, 15 samples were prepared and examined. The resin of sample 11 of the PAI 1 wire cracked during the testing process, so the overall test series of this wire contains measurement data of 14 samples. Figure 7 shows the measured values for each of the three wires tested in a boxplot diagram. For the PAI 1 wire, the lowest measured force was 914 N and the highest measured force was 1143 N. The range from the lower quartile to the upper quartile spans the range of 983 N to 1088 N. The mean and median are very close to each other with 1043 N for the mean and 1037 N for the median. For wire PAI 2, the lowest measured force was 630 N, whereas the highest measured value was 1243 N. The lower quartile could be measured at 805 N and the upper quartile at 1040 N. The range of the box is thus significantly higher than the values of the box of the PAI 1 wire. The mean value with a value of 919 N as well as the median with a value of 923 N are also significantly below the values for the PAI 1 wire. The lowest and highest measured force for the PEEK wire is 116 N and 277 N, respectively. The lower quartile has a value of 194 N, whereas the upper quartile has a measured value of 244 N. The mean and median values are very close to each other at 210 N and 203 N. It is striking that the mean value of the PEEK wire is about a factor of 5 smaller than the mean values of the two PAI wires.

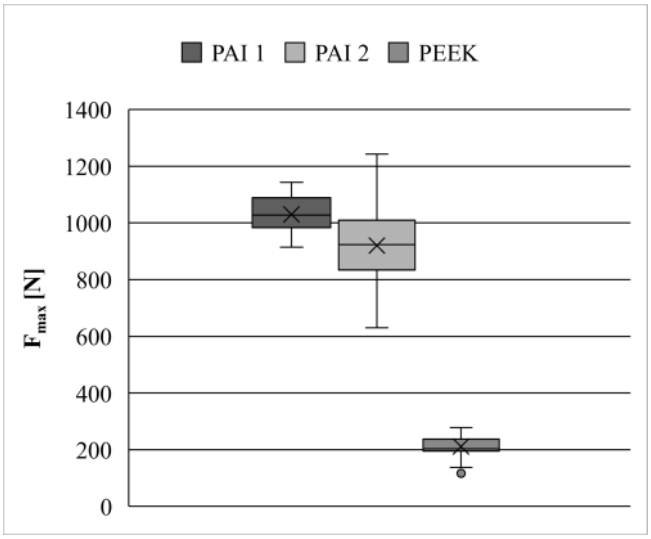

Figure 7: Display of the measured values in a boxplot diagram

The measurement results show that there is a significant difference in adhesion between an impregnation resin and wire insulations that differ in material. In particular, the adhesion of the PEEK-coated flat wire is significantly lower than that of PAI.

It is also noticeable that the measured values of the PAI 2 wire show a significantly greater scatter compared to the PAI 1 wire. This fact suggests that within one wire there may be high differences in the surface properties resulting in varying adhesion of the impregnating agent. One potential explanation lies in the production process of the enameled flat wire. One possible cause, for example, is that the solvent is not uniformly evaporated in the coating process, thus affecting the adhesion properties.

With regard to the developed test procedure, the high reproducibility of the measurement results shows that a valid method for determining adhesion has thus been created. Standard deviations of 62 N (PAI 1), 159 N (PAI 2) and 43 N (PEEK) support this statement.

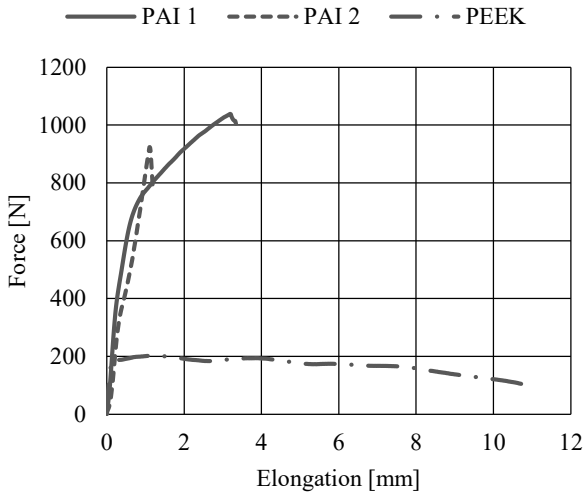

Figure 8: Exemplary force-elongation curves of three different wire samples

The force-elongation curve of one specimen from each of the three test series executed is shown in Figure 8. When looking at the PAI 1 curve, it is noticeable that the curve initially rises very steeply linearly, and the slope drops in the range between 700 N and 800 N. The maximum force at which the resin dissolves is 1037 N. The falling slope suggests that plastic deformation of the copper wire occurs here. The detachment of the resin therefore only occurs as soon as the specimen has left the elastic range. As a result of the plastic deformation, a significant reduction in the cross-section of the flat wire can be assumed during the test. Against the background outlined, it remains open what influence the reduction of the cross-section has on the adhesion of the resin and how this influences the test results. The curve of PAI 2 is also very steep. The detachment of the resin occurs here before the wire passes from the region of elastic to the region of plastic deformation. The fact that the PAI 1 wire already enters the plastic deformation range during the tensile test is also supported by the fact that the average length change at F_{max} is 3.56 mm, whereas this is only 1.09 mm for PAI 2. For the PEEK specimens, this value amounts to 0.88 mm. However, it should also be considered that the cross-section of the PAI 2 copper wire is about 57 % larger than that of the PAI 1 copper wire.

4. Conclusion

The choice of the right insulation system for electric motors, consisting of primary and secondary insulation, is one of the greatest challenges against the background of increasing voltage levels in electric drivetrains. The insulation on the flat copper wire for hairpin stators is the main focus here. To avoid aging effects at higher voltage levels, various insulation materials are used. The current trend is mainly towards PAI and PEEK as insulation materials. However, when choosing the insulation material, not only the electrical properties but also the interactions with the impregnating resin should be considered. In order for the resin to fulfill its requirements as secondary insulation, sufficient adhesion between wire insulation and resin is necessary. If the resin detaches from the wire insulation during operation due to vibration, cavities are created which favor partial discharge effects and thus lead to the failure of the drive unit in the long term.

Within the scope of this work, a method was developed to test and measure the adhesion between copper flat wires with different insulation materials and an impregnating agent. The tests carried out with three different insulated copper flat wires showed that the method is very well suited for reproducibly measuring the adhesion between resin and wire. It was also shown that there are significant differences in adhesion between the impregnating resin and different insulation materials. The adhesion on the insulation material PEEK is significantly lower than on PAI. It was also shown that differences in adhesion exist with the same insulation material, but from different manufacturers. The reasons for this observation cannot be clearly

identified. However, it is reasonable to assume that the wire manufacturing process varies. The process parameters in wire production thus have a strong influence on the properties of the insulated flat copper wire, which can be observed, for example, in fluctuating adhesion between wire and resin. The extent to which these fluctuations influence the properties in operation must be investigated further.

For future investigations, the measured values obtained must be evaluated in the context of the automotive application. So far, there is a lack of investigations that have made the acting forces between insulation material and impregnation resin quantifiable. The adhesion requirements, particularly with regard to service life tests, must be defined so that different insulation materials and impregnating resins can be evaluated with regard to use for automotive electric motors.

Acknowledgements

This work is part of the research project HaPiPro² (funding indicator: EFO-0011A) funded by the federal state of North Rhine-Westphalia.

References

[1] Moghadam, D.E., Herold, C., Zbinden, R., 2020. Electrical Insulation at 800 V Electric Vehicles, in: 2020 International Symposium on Electrical Insulating Materials (ISEIM). IEEE, pp. 115–119.

[2] Moghadam, D.E., Lange, J., 2020. The future of e-cars - will high-voltage systems become a new standard? JEC Composites Magazine, 30–33.

[3] Kampker, A., Heimes, H.H., Kawollek, S., Treichel, P., Kraus, A., 2020. Production Process of a Hairpin Stator, 2nd ed., Frankfurt am Main.

[4] Hagedorn, J., Sell-Le Blanc, F., Fleischer, J., 2018. Handbook of coil winding: Technologies for efficient electrical wound products and their automated production. Springer, Berlin, 306 pp.

[5] Moghadam, D.E., Herold, C., Zbinden, R., 62020. Effects of Resins on Partial Discharge Activity and Lifetime of Insulation Systems Used in eDrive Motors and Automotive Industries, in: 2020 IEEE Electrical Insulation Conference (EIC). 2020 IEEE Electrical Insulation Conference (EIC), Knoxville, TN, USA. 22.06.2020 - 03.07.2020. IEEE, pp. 221–224.

[6] DIN German Institute for Standardization. Winding wires - Test methods. Beuth Verlag GmbH 29.060.10.

[7] DIN German Institute for Standardization, 2021. Specifications for particular types of winding wires: Part 0-2: General requirements - Enamelled rectangular copper wire. Beuth Verlag GmbH 29.060.10.

[8] Wacker Chemie AG. Elastosil® RT 620 A/B: Technical Data Sheet. https://www.wacker.com/h/en-hu/medias/ELASTOSIL-RT-620-AB-en-2020.07.01.pdf. Accessed 21 August 2022.

[9] Elantas GmbH. ELAN-protect® UP 142: Technical Data Sheet. https://products.elantas.com/beckinsulation/productReport/ELAN-protect%C2%AE%C2%A0_UP_142.pdf?language=en&country=&download=productReport&productid=000002de&brandid=66958. Accessed 21 August 2022.

Biography

Prof. Dr.-Ing. Achim Kampker (*1976) is head of the chair “Production Engineering of E-Mobility Components” (PEM) of RWTH Aachen University and known for his co-development of the “StreetScooter” electric vehicle. Kampker also acts as member of the executive board of the “Fraunhofer Research Institution for Battery Cell Production FFB” in Münster. He is involved in various expert groups of the federal and state governments.

Dr.-Ing. Dipl. Wirt.-Ing. Heiner Hans Heimes (*1983) studied mechanical engineering with a focus on production engineering at RWTH Aachen University. From 2015 to 2019, he was head of the Electromobility Laboratory (eLab) of RWTH Aachen University and chief engineer of the newly established chair "Production Engineering of E-Mobility Components" (PEM). Since 2019, Dr.-Ing. Heimes has held the role of executive engineer of the PEM facility.

Benjamin Norbert Dorn (*1991) is chief engineer of the chair “Production Engineering of E-Mobility Components (PEM) of RWTH Aachen University. From 2017 to 2021 he was research associate at the PEM facility of which he has been responsible for the research group Electric Drive Production for the last two years. Since 2021, he has been responsible for the department production technology and organization.

Florian Brans (*1992) studied mechanical engineering and business administration at RWTH Aachen University. From 2019 to 2021, he was a research associate at the chair of “Production Engineering of E-Mobility Components” (PEM) of RWTH Aachen University. Since 2021, he has been responsible as group leader for the research group Electric Drive Production at PEM.

Henrik Christoph Born (*1994) is research associate at the chair of “Production Engineering of E-Mobility Components” (PEM) at RWTH Aachen University. He studied mechanical engineering and business administration with a focus on production engineering as well as corporate development and strategy the same university.